

Hydrothermal liquefaction of high- and low-lipid algae: Bio-crude oil chemistry

Feng Cheng^a, Zheng Cui^a, Lin Chen^b, Jacqueline Jarvis^c, Neil Paz^c, Tanner Schaub^c, Nagamany Nirmalakhandan^d, Catherine E. Brewer^{a,*}

^a Department of Chemical and Materials Engineering, New Mexico State University, P.O. Box 30001 MSC 3805, Las Cruces, NM 88003, USA

^b Department of Chemistry and Biochemistry, New Mexico State University, USA

^c Chemical Analysis and Instrumentation Laboratory, College of Agricultural, Consumer and Environmental Sciences, New Mexico State University, Las Cruces, NM 88003, USA

^d Department of Civil Engineering, New Mexico State University, USA

HIGHLIGHTS

- Algal lipid and protein content affect the composition and upgrading of HTL oils.
- *N. salina* bio-crude oils contain more fatty acids, amides, and aliphatic molecules.
- *G. sulphuraria* bio-crude oils have more N- and O-heteroatom aromatic molecules.
- Bio-crude oils recovered with lower-polarity solvents are better for upgrading.
- Carbohydrates should be removed prior to HTL, but N removed by catalytic upgrading.

ARTICLE INFO

Keywords:

Hydrothermal liquefaction

Bio-crude oil

Algae

High resolution FT-ICR MS

Heteroatom-containing compounds

ABSTRACT

The bio-crude oil produced from hydrothermal liquefaction (HTL) of a high-protein microalgae useful for wastewater treatment, *Galdieria sulphuraria*, was comprehensively characterized, and compared to that of a high-lipid microalgae useful for biofuel production, *Nannochloropsis salina*. HTL was conducted in a batch reactor at temperatures of 310–350 °C and reaction times of 5–60 min. Characterization methods included high-resolution Fourier transform ion cyclotron resonance mass spectroscopy (FT-ICR MS), fatty acid methyl ester (FAME) analysis by gas chromatography mass spectroscopy (GC/MS), proton nuclear magnetic resonance spectroscopy (¹H NMR), and Fourier transform infrared spectroscopy (FT-IR). Milder reaction conditions favored bio-crude oil yield and quality for *N. salina*, while more severe conditions (350 °C) were needed for *G. sulphuraria*. *N. salina*-derived bio-crude oil contained mainly C₁₄–C₁₈ fatty acid amides, while *G. sulphuraria*-derived bio-crude-oil had many N_{1.3}O_{0.2} hetero-atom compounds. FT-ICR MS showed that the aromaticity of hetero-compounds in *N. salina* bio-crude oil was higher due to *N. salina*'s higher carbohydrate content and the tendency of carbohydrate-derived molecules to condense at HTL conditions. FAME-GC/MS and ¹H-NMR results showed that stable fatty acid amides increased in *G. sulphuraria* bio-crude oil at higher temperatures as more protein-derived compounds combined with lipid-derived compounds. While N-containing and high molecular weight compounds are a concern for the upgrading of bio-crude oils obtained from high-protein algal biomass, removal of carbohydrates rather than removal of proteins as a pretreatment to HTL is recommended since carbohydrate-derived compounds are more likely to create highly aromatic hetero-compounds that are much more difficult to upgrade.

1. Introduction

Hydrothermal processing is one of the most competitive thermochemical conversion methods for wet biomass. Hydrothermal carbonization produces char-like solid at low temperatures (170–250 °C) [1],

hydrothermal liquefaction (HTL) produces bio-crude oil at moderate temperatures (250–370 °C), and hydrothermal gasification produces energy-rich gases at high temperatures (370–750 °C) [2]. As liquid fuels have higher energy density relative to solid fuels or syngas [3], many researchers have used HTL for conversion of wet biomass into bio-oils.

* Corresponding author.

E-mail address: cbrewer@nmsu.edu (C.E. Brewer).

<http://dx.doi.org/10.1016/j.apenergy.2017.08.105>

Received 7 April 2017; Received in revised form 27 May 2017; Accepted 12 August 2017

Available online 04 September 2017

0306-2619/ © 2017 Elsevier Ltd. All rights reserved.

Most components (lipids, proteins and carbohydrates) in algae can contribute to the formation of bio-crude oil, so bio-crude oil yields can exceed the original lipid content of the algae [4].

To date, most studies on the HTL of algae have focused on the optimization of operating conditions to improve bio-crude oil yields [5] and energy content/energy recovery [6]. Few studies have focused on the chemistry of bio-crude oils, which is imperative for upgrading the highly complex mixtures into finished products. Of particular concern for upgrading are oxygen, nitrogen, and ash [7]. Although bio-crude oils from HTL of algae generally have lower oxygen contents, lower moisture contents [8], and higher heating values (HHV) [9] than fast pyrolysis bio-oils from the conversion of lignocellulose biomass, algae contain more protein and, therefore, more nitrogen. Homogeneous [10] and heterogeneous [11] catalysts, and organic solvents [12], have been used in HTL to remove hetero-atoms in bio-crude oils, however, the yield and quality of the bio-crude oil is generally more influenced by the water itself [13]. As it nears its critical point at 374 °C and 22 MPa, water acts more like a non-polar solvent with lower density, a lower dielectric constant, and enhanced mass transfer. Under subcritical conditions (180–370 °C and 5–21 MPa), a variety of HTL reactions are catalyzed by H^+ or OH^- ions generated from the water molecules [8]. These reactions include hydrolysis, dehydration, decarboxylation, repolymerization, deamination [8], and Maillard reactions [14], which convert macromolecules (e.g. lipids, proteins [15] and carbohydrates [16]) into water-insoluble molecules, water-soluble molecules, non-condensable gases, and solid char [17].

The influences of algal composition on HTL have been well studied [18]. At HTL temperatures below 250 °C, lipids are hydrolyzed into various free fatty acids that make up the organic product phase. With increasing temperatures and reaction times, algal cell walls break, and proteins and some carbohydrates undergo deamination, decarboxylation, deoxygenation, and repolymerization. These reactions add heteroatom-containing organic compounds to the bio-crude oil phase [19]. Torri et al. [20] found that the HTL temperature for the highest bio-crude oil yield is much lower for high-lipid algal biomass than for high-protein or high-carbohydrate biomass. Higher temperatures also favor the transfer of heteroatom-containing compounds into the bio-crude oil.

Bio-crude oil's complexity has made it difficult to accurately describe and track changes in bio-crude oil chemistry. Ultrahigh resolution Fourier transform ion cyclotron resonance mass spectrometry (FT-ICR MS) has been used to characterize the chemical composition of fossil oils [21], bio-oils [22], and algal lipid extracts [23] for compounds across a wide range of molecular weights, the vast majority of which cannot be detected by gas chromatography mass spectroscopy (GC/MS) due to low volatility and spectral complexity [24]. Specifically, FT-ICR MS provides exceptionally high mass resolving power (e.g., $m/\Delta m_{50\%} = 400,000$ at m/z 400, where $\Delta m_{50\%}$ is the mass spectral peak width at half-peak height for mass m and charge z) and mass measurement accuracy in the range of 100–500 parts-per-billion [25]. This method enables the direct detection of thousands of organic compounds simultaneously and offers insight for feedstock selection, process optimization, and downstream processing [26]. Negative-ion mode FT-ICR MS has been used to characterize fast pyrolysis bio-oils [27] where highly oxygenated compounds (O_x and NO_x classes) are present [28]. By comparison, bio-crude oils from HTL of algae tend to contain fewer O-containing compounds but more N-containing compounds. In addition, highly oxygenated compounds tend to fractionate into the HTL aqueous phase, while nitrogen-containing compounds fractionate into the organic phase [24]. Therefore, positive-ion mode electrospray ionization (ESI) FT-ICR MS is beneficial for characterization of algal HTL bio-crude oils [29].

Nannochloropsis salina (hereafter *N. salina*) is one species of a genus of marine microalgae that has been well-studied for biofuel production due to its high lipid content [30]. *Galdieria sulphuraria* (hereafter *G. sulphuraria*) is an acidophilic red microalgae that recently has attracted attention as a potential species for wastewater treatment and biomass

production due to its wide tolerances for growth conditions and mixotrophic metabolism [31]. *G. sulphuraria* represents a low-lipid, high-protein algal biomass that may be a good candidate for recovering energy as liquid fuel from wastewater treatment, but for which there is little existing conversion data.

This study is one component of a multi-part study to evaluate yields, energy recovery, and chemistry of bio-crude oil produced from HTL of a high-protein *G. sulphuraria* relative to other biofuel candidate microalgae. The goal of this study is to identify HTL reaction conditions to convert *G. sulphuraria* into bio-crude oil more suitable for upgrading into “drop-in” transportation bio-fuels, where suitability is a function of the molecular weight, aromaticity, and heteroatom content. This is done by using a comprehensive suite of characterization methods on HTL bio-crude oils produced under varying operating conditions. Data from this study represents the first time that HTL light and heavy bio-crude oil chemistries from a high-lipid and high-protein algae species are compared directly.

2. Materials and methods

2.1. Algae production and hydrothermal liquefaction

A starter culture of *Nannochloropsis salina* (CCMP1776) was obtained from the Provasoli-Guillard National Center for Culture of Marine Phytoplankton (CCMP). The starter culture was expanded in 20 L carboys then transferred to an outdoor photobioreactor system (Solix Algredients, Fort Collins, CO), located at the NMSU Algal Growth Facility in Las Cruces, NM. The algae were grown in 200 L batch cultures in f/2 growth medium with 2% ocean salts. *Galdieria sulphuraria* (CCMEE 5778.1) was identified by the Culture Collection of Microorganisms from Extreme Environments (University of Oregon). The strain was grown in a modified cyanidium medium where the pH was adjusted to 2.5 with 10 N H_2SO_4 . The algae were grown in the same outdoor photobioreactor system using natural photoperiod and light intensity. The temperature in the enclosed growth bags was substantially hotter than the ambient air temperature. Algal cultures were harvested and concentrated by a custom-built high speed continuous centrifuge (AC26VHC, Type 265322CD, Pennwalt, India) at 15,000 rpm for 1–2 h with a flow rate of 8 L/min. Samples were stored at –20 °C prior to use. Algae biomass characterization methods and growth media composition are detailed in the [supplemental information](#).

HTL experiments were performed in a 1.8 L Model 4572 stainless steel batch reactor with a Model 4848B controller unit (Parr Instrument Co., Moline, IL). Algae slurries of different solid concentrations (5 and 10 wt.%) were converted at temperatures of 310, 330 and 350 °C and reaction times of 5, 30, and 60 min. The HTL products: light bio-crude oil (LBO), heavy bio-crude oil (HBO), char, and aqueous phase, were recovered using a hexane extraction procedure, followed by char rinsing with dichloromethane (DCM), and then solvent evaporation at 50 °C using a rotary evaporator. The hexane-soluble product was designated as LBO; the hexane-insoluble, DCM-soluble fraction was designated as HBO. Both LBO and HBO fractions were stored in sealed glass containers at 4 °C prior to analysis. The hexane and DCM were analytical grade (Pharmco-Aaper, Shelbyville, KY). Yield and reaction ordinate calculations are shown in the [supplemental information](#).

2.2. Characterization of bio-crude oils by FT-ICR-MS

Bio-crude oil samples were diluted in 1:1 chloroform:methanol (HPLC grade, Sigma-Aldrich, St. Louis, MO) to a concentration of 1 mg/mL, then to a final concentration of 250 µg/mL in 1:3 chloroform:methanol with 1% formic acid. Positive-ion electrospray ionization ((+) ESI) FT-ICR MS was performed with a hybrid linear ion trap, 7T FT-ICR mass spectrometer (LTQ FT, Thermo Fisher, San Jose, CA) equipped with an Advion TriVersa NanoMate system (Advion, Ithaca, NY). Multiple 300 individual time-domain transients were co-added,

Hanning-apodized, zero-filled, and fast Fourier transformed prior to frequency conversion to mass-to-charge ratio to obtain the final mass spectrum [32]. The mass resolving power was $m/\Delta m_{50\%} = 400,000$ at m/z 400. All transient lengths were 3 s. Data were analyzed and peak lists generated with PetroOrg® software [33]. Internal mass calibration of mass spectra was based on homologous series whose elemental compositions differ by integer multiples of 14.01565 Da (i.e., CH_2) [34]. Elemental formulae were assigned to peaks $> 10\sigma$ RMS noise.

2.3. Characterization of bio-crude oils by FAME analysis with GC-MS

Fatty acid methyl esters (FAME) in the bio-crude oils were quantified using an Agilent 6890 gas chromatograph with a 5973i mass selective detector (GC-MS) equipped with a DB-WAX, 30 m \times 0.25 mm ID \times 0.25 μm film thickness capillary column (Agilent, Santa Clara, CA). An internal standard stock solution of 13:0 methyl tridecanoate (Sigma Aldrich, St. Louis, MO) was prepared in HPLC grade hexane (Sigma Aldrich, St. Louis, MO) to a concentration of 10 mg/mL. Each bio-crude oil sample was prepared by adding 20 μL of the internal standard solution to 200 μL of 1 M HCl/methanol (20 μL standard solution/mg sample). Samples were esterified at 80 $^\circ\text{C}$ for 30 min. After cooling to ambient conditions, 1 mL of HPLC-grade hexane was added to the sample, diluted 1:20, and injected for analysis. A calibration curve was generated using a 37 component FAME mixture (Sigma Aldrich, St. Louis, MO). GC-MS parameters included 2- μL splitless injection with a constant flow rate of 1 mL/min helium, inlet temperature of 250 $^\circ\text{C}$, and the transfer line temperature of 275 $^\circ\text{C}$. The oven program started at 100 $^\circ\text{C}$, ramped at 25 $^\circ\text{C}/\text{min}$ to 200 $^\circ\text{C}$ for 1 min, ramped at 5 $^\circ\text{C}/\text{min}$ to 230 $^\circ\text{C}$ for 7 min, and ramped at 5 $^\circ\text{C}/\text{min}$ to 240 $^\circ\text{C}$ for 2 min. The quadrupole temperature was 150 $^\circ\text{C}$ and the ion source temperature was 250 $^\circ\text{C}$.

2.4. Characterization of bio-crude oils by ^1H NMR

Functional groups in the bio-crude oils were semi-quantitatively analyzed at room temperature by nuclear magnetic resonance spectroscopy (NMR) using an Oxford 300 MHz NMR (Varian, Palo Alto, CA). Bio-crude oil (30 mg) was dissolved in 600 μL of deuterated chloroform (CDCl_3) (Aldrich 99%) with 0.03% (v/v) tetramethylsilane (TMS) as an internal standard. The ^1H NMR spectra were acquired at 300 MHz with pulse delay of 1 s, a 45 $^\circ$ pulse angle, spectral width of 4800 Hz, spinner frequency of 20 Hz, and 32 scans per ^1H spectrum.

2.5. Characterization of algae biomass and bio-crude oils by FT-IR

Chemical functional groups in the algal biomass and bio-crude oils were characterized by Fourier transfer infrared spectroscopy (FT-IR) using a Spectrum Two FT-IR spectrophotometer (PerkinElmer, MA, USA) equipped with a crystal reflectance cell. Transmittance mode was used over a range of 4000–400 cm^{-1} at a resolution of 4 cm^{-1} with 10–30 scans [35]. For the LBO samples, approximately 1–2 mg was placed as a drop onto the crystal surface and then pressed into the crystal head. For the feedstock and HBO samples, a small amount was ground into fine powder and placed onto the crystal surface. At least two replicates were taken for each sample.

3. Results and discussion

3.1. Algae feedstock composition and bio-crude oil yields

The composition of the algae feedstocks, a summary of the HTL reaction conditions, and the bio-crude oil yields are shown in Tables 1 and 2, respectively. *N. salina* biomass contained approximately 20 wt.% lipid and 14 wt.% protein, and had LBO and HBO yields of 40–54 wt.% and 3–9 wt.% on a dry feedstock basis, respectively. The highest LBO yield was achieved at 310 $^\circ\text{C}$ and 60 min with an algal solid loading

Table 1
Composition of algal feedstocks.

Algal species	<i>N. salina</i> CCMP 1776	<i>G. sulphuraria</i> CCME 5587.1
Proximate analysis		
Moisture content wt.% ^a	28.5 \pm 0.9	31.0 \pm 0.3
Ash content wt.% ^b	7.3 \pm 0.5	10.4 \pm 0.5
HHV MJ/kg ^b	27.0 \pm 0.9	20.5 \pm 1.0
Elemental analysis wt.%^b		
Carbon	55.9 \pm 0.3	44.5 \pm 0.2
Hydrogen	7.8 \pm 0.3	7.7 \pm 1.3
Nitrogen	2.8 \pm 0.3	9.5 \pm 0.2
Sulfur	2.8 \pm 0.2	3.0 \pm 0.6
Oxygen ^d	23.3 \pm 0.6	25.4 \pm 2.6
Biochemical analysis wt.%^c		
Lipid	19.7 \pm 1.3	5.5 \pm 0.7
Protein	13.5 \pm 1.2	45.3 \pm 1.0
Carbohydrate	22.9 \pm 1.1	14.5 \pm 1.0

^a Wet basis.

^b Dry basis.

^c Dry ash free basis.

^d By difference.

Table 2
Yields of light (hexane-soluble) bio-crude oil (LBO) and heavy (hexane-insoluble, DCM-soluble) bio-crude oil (HBO) from HTL of *G. sulphuraria* and *N. salina*. Each reaction was run twice. \pm = standard deviation. Log R_t = logarithmic reaction ordinate.

Solid algae content (wt.% ^a)	Reaction temperature ($^\circ\text{C}$)	Reaction time (min)	Log (R_t)	LBO yield (wt.%) ^a	HBO yield (wt.%) ^a
<i>G. sulphuraria</i> CCME 5587.1					
5	310	60	8.03	18.1 \pm 1.2	5.0 \pm 1.1
5	350	5	8.55	20.1 \pm 0.8	8.9 \pm 0.6
5	330	60	8.62	19.6 \pm 1.0	6.1 \pm 0.4
5	350	30	8.97	22.6 \pm 2.7	8.4 \pm 2.0
5	350	60	9.21	27.5 \pm 0.7	3.3 \pm 2.4
10	350	60	9.21	21.7 \pm 0.2	9.7 \pm 1.5
<i>N. salina</i> CCMP 1776					
5	310	5	7.35	49.6 \pm 1.0	9.4 \pm 4.2
5	310	30	7.78	51.8 \pm 0.2	5.4 \pm 0.0
5	310	60	8.03	54.3 \pm 1.5	4.8 \pm 1.4
10	310	60	8.03	52.4 \pm 0.6	2.8 \pm 0.5
5	330	60	8.62	52.8 \pm 1.7	3.7 \pm 1.3
5	350	60	9.21	40.0 \pm 1.3	3.9 \pm 1.1

^a Dry feedstock basis.

content of 5 wt.%. *G. sulphuraria* biomass contained approximately 5 wt.% lipid and 45 wt.% protein, and had LBO and HBO yields of 18–28 wt.% and 3–10 wt.%, respectively. The highest LBO yield was achieved at 350 $^\circ\text{C}$ and 60 min with an algal solid loading content of 5 wt.%. The compounds in bio-crude oil are intermediate products of HTL [36]. As temperatures increase, more protein-derived and carbohydrate-derived compounds are formed as low-polarity heterocyclic compounds via Maillard [37] and rearrangement reactions, leading to bio-crude oil yield increases [20]. As temperatures increase further, bio-crude oil compounds crack into gaseous CO_2 and NH_3 , or re-polymerize into solid (poly-aromatic) products, resulting in bio-crude oil decreases [5]. These two phenomena were seen at 350 $^\circ\text{C}$ with bio-crude oil yield increases for *G. sulphuraria* and bio-crude oil yield decreases for *N. salina*.

3.2. Bio-crude oil composition by (+) ESI FT-ICR MS

Results from (+) ESI FT-ICR MS observations of heteroatom-containing compounds in the bio-crude oils are shown in Figs. 1–7 and supplemental information Figs. S1–S13.

For *N. salina*-derived HTL bio-crude oils made under the optimal

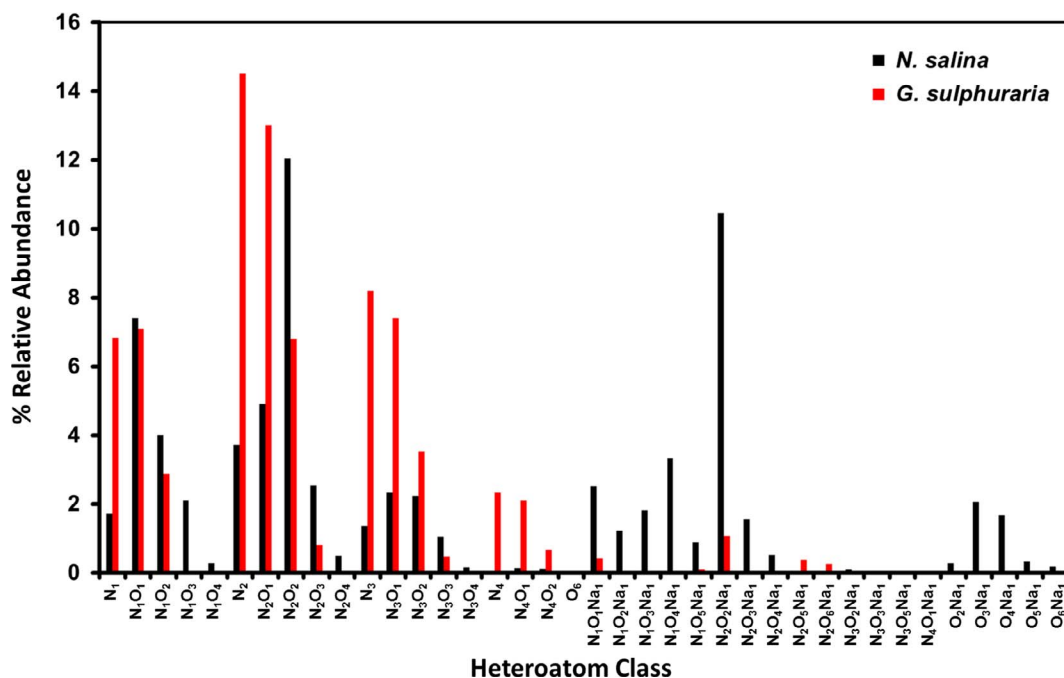


Fig. 1. Heteroatom class distribution of LBO from HTL of 5 wt.% both algal species under 310 °C and 60 min derived from positive-ion ESI FT-ICR MS.

operating conditions (5 wt.%, 310 °C, and 60 min, or Log R = 8.03), the most abundant heteroatom classes (of the 66 heteroatom classes observed) were N_2O_2 , $N_2O_2Na_1$, N_1O_1 , N_2O_1 , N_1O_2 , N_2 . Combined, these six classes accounted for more than 40% of the summed abundance of the hetero-compounds. Within the N_2O_2 , $N_2O_2Na_1$, and N_1O_1 heteroatom classes, more than 50% consist of fatty acid amides with double bond equivalents (DBE) of 2 or 3. Two of the most abundant groups of hetero-compounds were $C_{38-41}H_{74-82}N_2O_2$ with 2 DBE and $C_{20}H_{39}N_1O_1$ with 2 DBE.

For *G. sulphuraria* HTL bio-crude oils made under the optimal operating conditions (5 wt.%, 350 °C and 60 min, or Log R = 9.21), the most abundant heteroatom classes (of the 40 observed) were N_2 , N_2O_1 , N_2O_2 , N_3O_1 , N_3 , N_1 , and N_1O_1 . These classes contributed more than 60% of the summed abundance of the hetero-compounds. *G. sulphuraria* bio-crude oil shows a wide compound distribution of over 5100 different hetero-compounds at similar concentrations. Most of the hetero-compounds are heterocyclic aromatics, specifically

$C_{23-29}H_{32-41}N_{1-3}O_{0-2}$ with DBE of 8–12, indicating that protein- and carbohydrate-derived compounds have undergone Maillard reactions, rearrangement, cyclization, and aromatization [38].

3.2.1. Effects of algal species

Bio-crude oils from HTL of *N. salina* and *G. sulphuraria* contain $N_{1-3}O_{0-3}$ classes in common (Fig. 1). The *G. sulphuraria* bio-crude oil contains a higher relative abundance of nitrogen-containing classes (e.g. N_1 , N_2 , N_2O_1 , and N_3) due to *G. sulphuraria*'s higher protein content, consistent with the results of Dandamudi et al. [39], whereas the *N. salina* bio-crude oil contains a higher relative abundance of sodiated species and oxygenated species due to *N. salina*'s higher lipid and carbohydrate contents (see examples in Fig. S1). Fig. 2 shows that *N. salina* and *G. sulphuraria* bio-crude oils have similar compositions in terms of carbon number and DBE for the N_1 , N_2 , N_3 , N_1O_1 , N_2O_1 , and N_3O_1 classes. The main compounds are aromatic species (DBE ≥ 4) ranging from C_{10} to C_{40} . Both carbon number and DBE increase with increasing

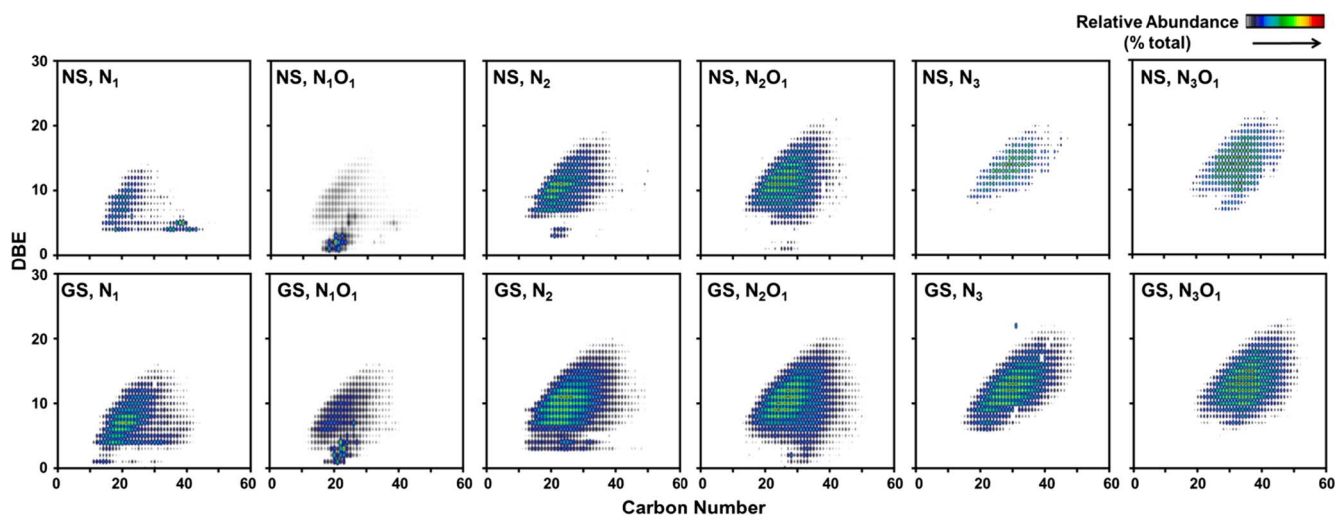


Fig. 2. Color-coded abundance-contoured plots of DBE versus carbon number for heteroatom classes in LBOs from 5 wt.% of both algal species under 310 °C and 60 min derived from positive-ion ESI FT-ICR MS.

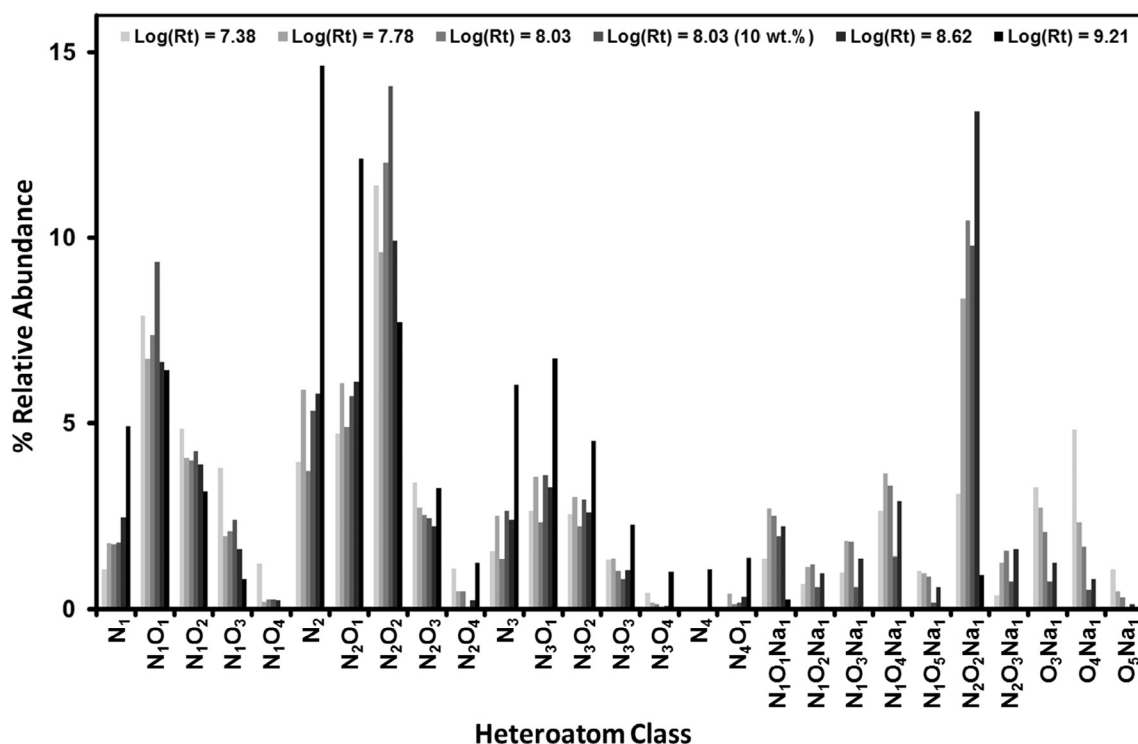


Fig. 3. Heteroatom class distribution for *N. salina* LBO under different Log (R_t) (operating conditions ranging from 310 °C for 5 min to 350 °C for 60 min.) derived from positive-ion ESI FT-ICR MS.

number of nitrogen atoms, indicating that saccharides and amino acids have rearranged into heterocyclic compounds with relatively high aromaticity; previous studies showed that algal heteroatoms form complex aromatic structures at temperatures ≥ 310 °C [38,40].

For the N_1 class, *N. salina* bio-crude oil contains more species with DBE > 4, such as alkyl-substituted pyrroles, pyridines, and indoles, with additional double bonds in the alkyl chain [24,41], relative to the

G. sulphuraria bio-crude oil which has higher degrees of alkylation. For the N_2 class, the compositional space (C_{13} – C_{39} and DBE of 4–19) of hetero-components in the *N. salina* bio-crude oil is narrower than that in the *G. sulphuraria* bio-crude oil (C_{12} – C_{48} and DBE of 3–18), indicating less hetero-compound diversity within the *N. salina* bio-crude oil. The most abundant components in the *N. salina* bio-crude oil have DBE three higher than those in the *G. sulphuraria* bio-crude oil, indicating

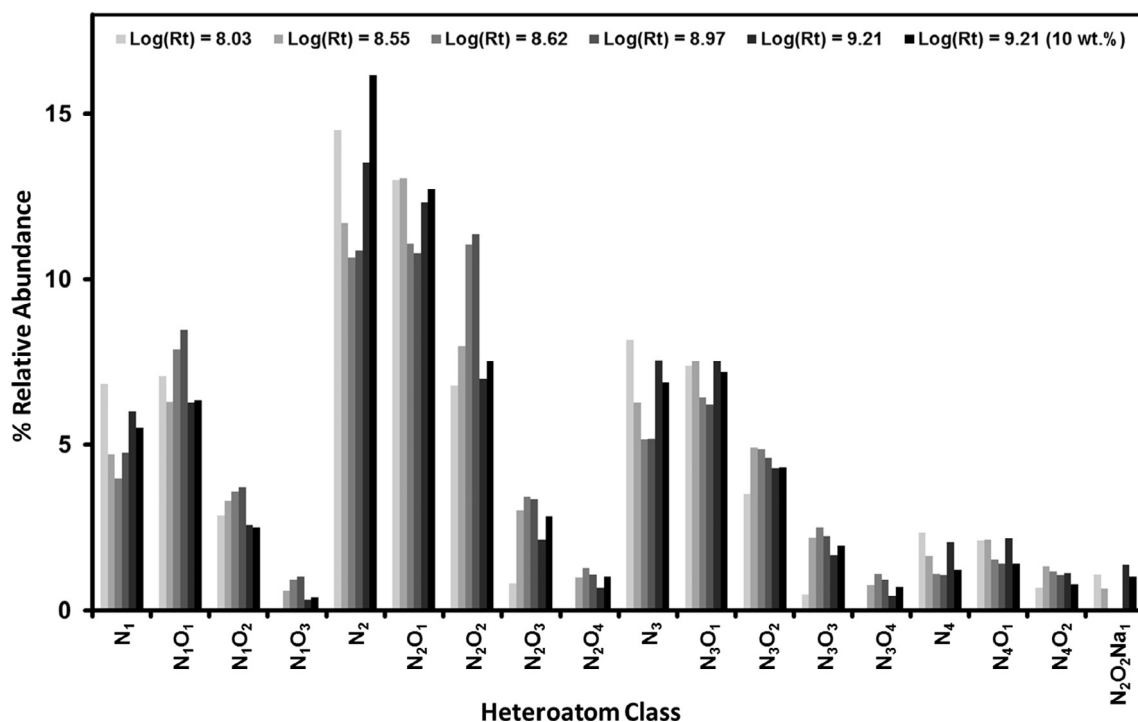


Fig. 4. Heteroatom class distribution for *G. sulphuraria* LBO under different Log (R_t) (operating conditions ranging from 310 °C for 60 min. to 350 °C for 60 min.) derived from positive-ion ESI FT-ICR MS.

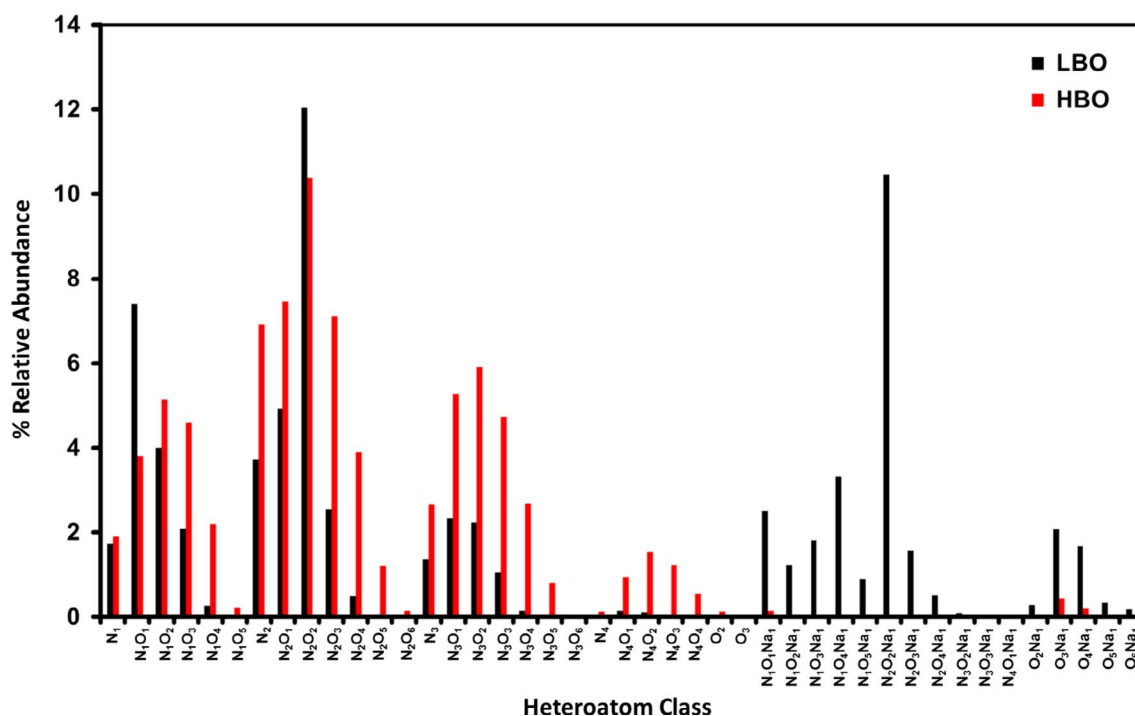


Fig. 5. Heteroatom class distribution for 5 wt.% *N. salina* LBO and HBO under 310 °C and 60 min derived from positive-ion ESI FT-ICR MS.

the presence of an additional aromatic ring in the core structure. Some examples of compounds in this class are alkyl-substituted quinoxaline or phenazine, and multiple-ring imidazole derivatives [24]. This can be caused by the lower nitrogen content and higher carbohydrate content in the *N. salina* feedstock, contributing to formation of heterocyclic compounds with higher aromaticity [38,42,43]. For the N_3 class, the *N. salina* bio-crude oil had lower relative abundance ($< 2\%$) than the *G. sulphuraria* bio-crude oil ($> 8\%$), with slightly higher observable DBE, 9–18 vs. 5–17, and similar carbon number ranges: 16–46 and 15–47, respectively. The main structures for both algae species in this class

were alkyl-substituted pyridyl-piperazines, and alkylated amine-substituted pyridines and imidazoles [24].

Within the N_1O_1 class, low-DBE (< 4) species were more abundant in the *N. salina* bio-crude oil due to the higher concentration of fatty acid amides from reactions of fatty acids with protein-derived compounds [44]. In both of the bio-crude oils, species with DBE of 4–7 and carbon numbers of 17–23 indicate the presence of aromatic amides [24] or oxygenated, nitrogen-heteroatom aromatic compounds. For the N_3O_1 class, the bio-crude oils had a similar pattern as the N_3 class, albeit with a shift to slightly higher DBE, which may be caused by the addition of

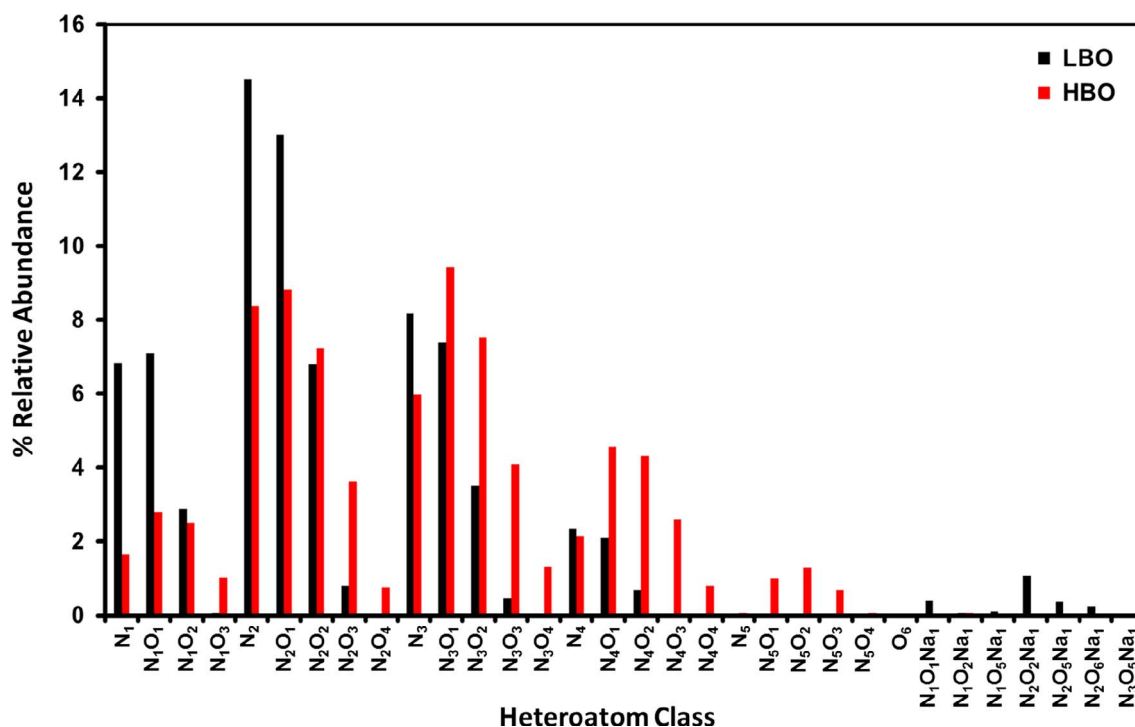


Fig. 6. Heteroatom class distribution for 5 wt.% *G. sulphuraria* LBO and HBO under 310 °C and 60 min derived from positive-ion ESI FT-ICR MS.

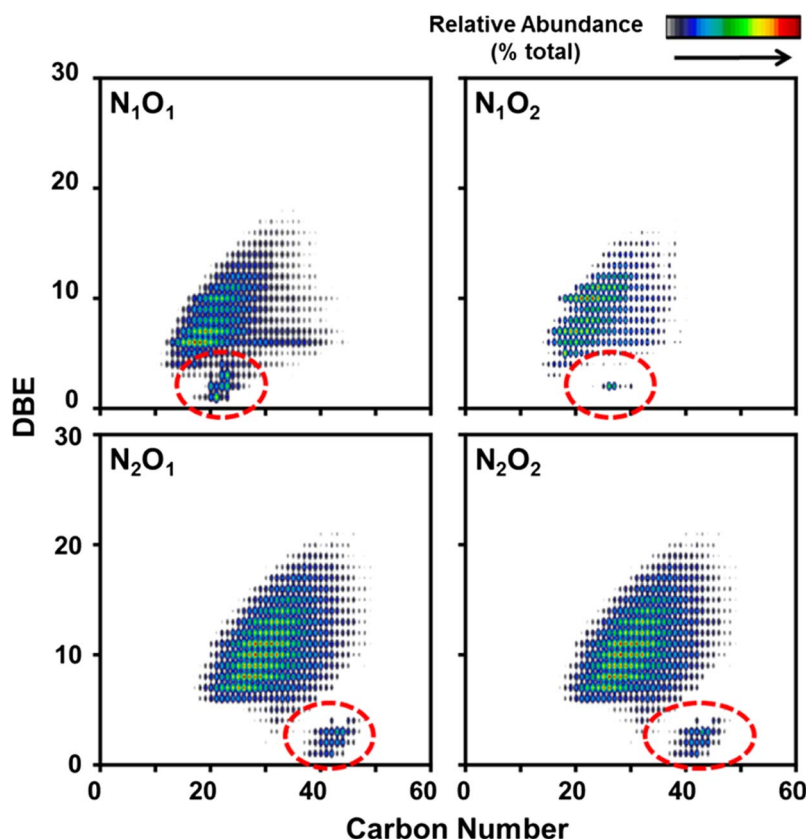


Fig. 7. Color-coded abundance contour plots of DBE versus carbon number for heteroatom classes in *G. sulphuraria* LBO made at 350 °C and 60 min derived from positive-ion ESI FT-ICR MS. Red cycles indicate the presence of fatty acids and amides. (For interpretation of the references to color in this figure legend, the reader is referred to the web version of this article.)

a C=O functional group to the N_3 species (through oxidation) or the addition of furans [24].

Regardless of algal species, carbohydrates contribute to the generation of highly cyclic compounds, the precursors of char [45]. Separating carbohydrates from algal feedstock prior to HTL is a potential method to improve the quality of algae-derived bio-crude oils [46].

3.2.2. Effects of HTL operating conditions

Slight increases in DBE (1–2) for most heteroatom classes were observed with increasing HTL temperatures, implying that more dehydrogenation via cyclization and aromatization occurred (Figs. S2 and S3). Almost no change in the compositional space was seen with varying reaction time (Figs. S4 and S5). This implies that reaction time affected overall bio-crude oil yield but not composition. Solid algae content (5 wt.% vs. 10 wt.%) also had little effect on the compositional spaces of heteroatoms for either algal species (Figs. 3 and 4, S6 and S7). For *N. salina* bio-crude oils made at 350 °C and 60 min (Fig. 3, $\log(R_f) = 9.21$), there is a noticeable decrease in the relative abundance of sodiated heteroatom classes ($N_{0-2}O_{1-5}Na_1$) and an increase in non-sodiated classes. Fig. S1 shows that most of sodiated species are long aliphatic chains (C_{10} – C_{40}) with low DBE (1–2). This indicates that fatty acids combine with amino acids or saccharides at lower temperatures, while rearrangement, Maillard [37], and dehydrogenation reactions form high DBE heterocyclic aromatic compounds (e.g. indoles, quinolines [47] and phenol derivatives [48]) at higher temperatures, consistent with the results of Tang et al. [49].

3.2.3. Differences between light and heavy bio-crude oils

The LBO and HBO derived from *N. salina* contain similar heteroatom classes, but differ in relative abundances and more sodiated species in the LBO (Fig. 5). In general, for any given number of nitrogen atoms, the number of oxygen atoms in the HBO is higher than in the LBO. A similar pattern was observed for the LBO and HBO from *G. sulphuraria* (Fig. 6), indicating that the formation of heavy bio-crude oil can be

attributed to the participation of oxygen-containing compounds. In addition, especially for *G. sulphuraria*, HBO contained higher relative abundances of heteroatom classes with > 3 heteroatoms relative to LBO. N_4 , N_4O_1 , and N_4O_2 classes were present in HBO at > 1% relative abundance but were not seen in LBO. For any given DBE value, the compositional space for LBO is more diverse in terms of carbon number, likely due to the higher degree of alkylation within LBO than within HBO (Figs. S8 and S9). For any given carbon number, LBO has lower DBE than HBO, suggesting that condensation and cyclization of heteroatom-containing components mark the transition between LBO (hexane soluble, easier to upgrade to hydrocarbons) and HBO (hexane insoluble) [50].

3.2.4. Characteristic structures of heteroatom classes

Figs. S10–S13 show a consistent compositional space feature in bio-crude oils: carbon number tends to increase with increases in the number of oxygen atoms while DBE tends to increase with increases in the number of nitrogen atoms. Observing chemical reactions that mark the transition from one heteroatom class to another is impossible in mixtures as complex as bio-crude oil. However, from theory, specific reactions have expected outcomes that can be considered in combination for potential reaction mechanisms. Decarboxylation removes one carbon and two oxygen atoms, and reduces DBE by one. Deamidation removes one nitrogen and one oxygen atom and increases DBE by one. Dehydration removes one oxygen atom and increases DBE by one. Amidation and Maillard reactions increase the numbers of carbon, nitrogen and oxygen atoms, and generally increase DBE. Overall, as nitrogen and oxygen contents increase ($N_{1-3}O_{0-3}$ classes), the compounds continue to be primarily heterocyclic aromatic compounds with higher DBE and larger carbon numbers.

3.3. Bio-crude oil composition by FAME GC-MS

The distributions of fatty acid methyl esters (FAME) found in the

Table 3Fatty acid methyl ester (FAME) distribution in *N. salina* biomass, LBO, and HBO under different operating conditions. All data reported as percentages on a dry, ash-free feed basis.

Sample	Log (R_t) ^a	Total FAME	C14:0	C14:1	C16:0	C16:1	C18:0	C18:1n9t	C18:1n9c	C18:2n6t	C18:2n6c	C20:5n3	Other lipids ^b
Biomass		20.65	1.01	0.56	6.23	4.12	0.41	1.30	2.55	0.53	0.53	1.46	1.95
LBO	7.35	26.50	1.51	0.83	9.44	7.07	0.80	1.99	3.97	0.41	0.05	0.00	0.43
LBO	7.78	25.56	1.45	0.78	9.89	6.48	0.85	1.84	3.54	0.31	0.07	0.01	0.34
LBO	8.03	23.65	1.39	0.73	8.99	6.20	0.81	1.72	3.30	0.14	0.06	0.01	0.3
HBO	8.03	0.41	0.01	0.00	0.19	0.11	0.01	0.02	0.05	0.00	0.00	0.00	0.02
LBO (10 wt.%)	8.03	22.65	1.26	0.66	8.30	5.48	0.80	1.50	2.97	0.16	0.05	0.01	1.46
LBO	8.62	23.87	1.39	0.76	8.70	6.37	0.87	1.79	3.54	0.10	0.07	0.00	0.28
LBO	9.21	16.91	1.04	0.55	6.25	4.52	0.70	1.25	2.31	0.05	0.04	0.00	0.2

^a Log (R_t) = 7.35, 7.78, 8.03, 8.62, and 9.21 correspond to HTL conditions of 310 °C and 5 min, 310 °C and 30 min, 310 °C and 60 min, 330 °C and 60 min, and 350 °C and 60 min, respectively.

^b Calculated by difference.

Table 4Fatty acid methyl ester (FAME) distribution in *G. sulphuraria* biomass, LBO and HBO under different operating conditions. All data reported as percentages on a dry, ash-free feed basis.

Sample	Log (R_t) ^a	Total FAME	C14:0	C14:1	C16:0	C16:1	C18:0	C18:1n9 t	C18:1n9 c	C18:2n6 t	C18:2n6 c	Other lipids ^b
Biomass		5.00	0.02	0.04	1.11	0.02	0.40	0.09	0.18	1.23	1.23	0.68
LBO	8.03	1.12	0.01	0.01	0.44	0.06	0.14	0.06	0.12	0.17	0.05	0.06
LBO	8.55	1.25	0.01	0.01	0.52	0.02	0.19	0.07	0.13	0.14	0.09	0.07
LBO	8.62	1.15	0.02	0.01	0.50	0.07	0.16	0.07	0.13	0.08	0.05	0.06
LBO	8.97	1.42	0.02	0.02	0.63	0.05	0.21	0.08	0.17	0.10	0.07	0.07
LBO	9.21	2.52	0.07	0.02	1.15	0.30	0.27	0.16	0.29	0.13	0.04	0.09
HBO	9.21	0.24	0.00	0.00	0.11	0.03	0.02	0.01	0.03	0.01	0.00	0.03
LBO (10 wt.%)	9.21	1.06	0.01	0.02	0.44	0.01	0.18	0.09	0.17	0.06	0.02	0.06

^a Log (R_t) = 8.03, 8.55, 8.62, 8.97, and 9.21 correspond to HTL conditions of 310 °C and 60 min, 350 °C and 5 min, 330 °C and 60 min, 350 °C and 30 min, and 350 °C and 60 min, respectively.

^b Calculated by difference.

algal biomass and in the esterified bio-crude oils are shown in Tables 3 and 4. FAME content in the *N. salina* biomass was 20.6 wt.%, which is consistent with the measured lipid content. Total FAME content in *N. salina* bio-crude oils decreased from 26.5 to 16.9 wt.% with increasing HTL temperature, and decreased from 26.5 to 23.6 wt.% when the reaction time was lengthened from 5 to 60 min, respectively. The decrease in FAME content is attributed to the decomposition, polymerization, and rearrangement of fatty-acid-like compounds [51], as supported by the increase in gas yields and the heavier heterocyclic aromatic compounds found by FT-ICR MS with increasing log (R_t). FAME content in the *G. sulphuraria* biomass was 5.0 wt.% and < 2.5 wt.% in the bio-crude oils. Within the bio-crude oils, total FAME content increased with increasing reaction severity, reaching 2.5 wt.% at 350 °C and 60 min (Table 4). FT-ICR MS results indicate that there are several different fatty acid amides present as N_1O_1 , N_1O_2 , N_2O_1 and N_2O_2 heteroatom classes (Fig. 7). Fatty acid amides are likely produced as protein-derived compounds (amino acids and amines) form at higher temperature, dissolve into the organic phase, and combine with fatty acids. This process helps to stabilize the fatty acids derivatives at the higher temperatures [49,52]. Very little FAME (< 0.4 wt.%) was detected in the HBO from either algal species.

In the *N. salina* biomass, the most abundant FAMES were palmitic acid (C16:0), palmitoleic acid (C16:1), oleic acid (C18:1n9c), elaidic acid (C18:1n9t), myristic acid (C14:0), stearic acid (C18:0), myristoleic acid (C14:1), eicosapentaenoic acid (C20:5n3), linolelaidic acid (C18:2n6t), and linoleic acid (C18:2n6c)—results that are consistent with Wang et al. [53]. During HTL, concentrations of eicosapentaenoic, linolelaidic and linoleic acids substantially decreased as they reacted with carbohydrate-derived compounds to form heterocyclic fatty acid derivatives, or as they decomposed into alkanes or alkenes via decarboxylation [54]. Within the *N. salina* bio-crude oils, FAME distributions were consistent at different operating conditions and were similar to the FAME distributions in the feedstock, except for the largest and most unsaturated FAMES, shown in Fig. S14. Poly-unsaturated C18 fatty acids are less stable at more severe HTL conditions, whereas saturated

C16 and C14 fatty acids can withstand higher temperatures for longer times. Similar results were observed by Patil et al. [55] and Brown et al [42].

In the *G. sulphuraria* biomass, the most abundant FAMES were linolelaidic, linoleic, palmitic, and stearic acids. During HTL, the concentrations of linolelaidic, linoleic, and stearic acids decreased, while that of palmitic acid increased. The FAME component distributions for the *G. sulphuraria* bio-crude oils were also generally consistent throughout different operating conditions. The most abundant FAMES were palmitic, stearic, oleic, linolelaidic, elaidic, palmitoleic, linoleic, heptadecanoic (C17:0), myristic, myristoleic, and pentadecanoic (C15:0) acids, shown in Fig. S15. As reaction conditions became more severe, the concentrations of linoleic, linolelaidic, and stearic acids decreased rapidly, while the concentrations of palmitic, palmitoleic, and myristic acids increased. HBO for both algal species had higher relative concentrations of C16 acids (palmitic and palmitoleic) and lower relative concentrations of C18 acids (stearic, elaidic, and oleic), as shown in Figs. S16 and S17.

The composition and quantity of fatty acids are more important for the LBO yield and quality from *N. salina* than from *G. sulphuraria*; as such, optimization efforts for *G. sulphuraria* HTL should focus on the reaction mechanisms for proteins and carbohydrates rather than for fatty acids. The stabilizing effect of protein-derived compounds on the fate of fatty acid derivatives during HTL suggests that protein (but not carbohydrate) content should be retained in the feedstock prior to HTL with nitrogen atoms being removed during downstream catalytic processes.

3.4. Bio-crude oil composition by ¹H NMR

The ¹H NMR spectra and integrated peak area spectral distributions for the LBO and HBO from *N. salina* and *G. sulphuraria* are shown in Fig. 8, and Tables 5–8. The most prominent peaks in Fig. 8c) are located at 0.78–0.80 ppm and 1.18 ppm, indicating the abundance of aliphatic methyl protons and methylene protons in alkyl chains [56],

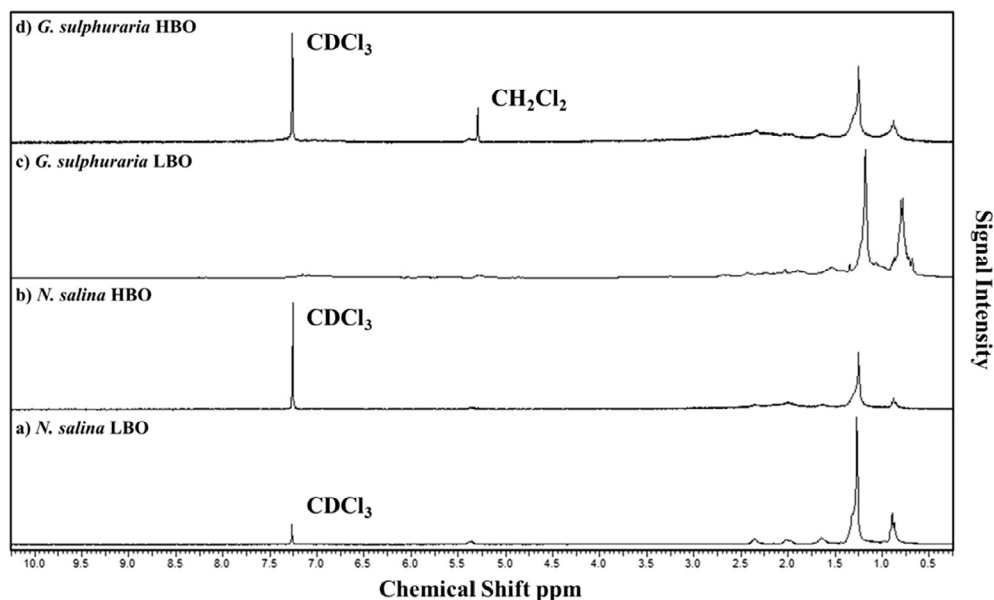


Fig. 8. ^1H NMR spectra from HTL of 5 wt.% both algal species under 310 °C and 60 min.

respectively, in the *G. sulphuraria* LBO. Similarly, the most prominent peaks in Fig. 8a) are located at 0.86–0.88 ppm and 1.26 ppm, indicating similar aliphatic functionalities in the *N. salina* LBO. Apart from these two primary peaks, the LBO spectra from both algae species have smaller peaks at 1.5–3.0 ppm, representing aliphatic protons in the α - or β -positions of unsaturated bonds (e.g. acetylenic, benzylic, allylic compounds), and in N- and O-containing functional groups in straight/branched amides and heterocyclic compounds [57]. The few protons resonating at 5.3 ppm in both LBO correspond to a small amount of non-conjugated olefinic protons, namely phenolic hydroxyl groups [58]. Little peak area is present in the 3.0–4.4 ppm range, characteristic of methoxyl ($-\text{CH}=\text{O}-$ and $-\text{CH}_2-\text{O}-$) functionalities [59], the 6.0–8.0 ppm range, characteristic of aromatic/heteroatom-aromatic functionalities [59], or the 8.0–10.0 ppm range, characteristic of aldehydes [56] (Tables 5–8).

In general, protons from aliphatic functionalities (0.5–1.5 ppm) contribute positively to bio-crude oil quality. At mild conditions, the relative percentage of aliphatic protons in LBO and HBO from *N. salina* is higher. As the HTL reaction conditions become more severe, aliphatic compounds are converted into heteroatom-containing, non-conjugated and aromatic compounds, as indicated by the higher percentage of protons in the 3.0–4.4 ppm, 4.4–6.0 ppm, and 6.0–8.0 ppm ranges (Tables 5 and 6). In contrast, the percentage of aliphatic protons in LBO from *G. sulphuraria* increases with more severe reaction conditions

(Table 7), mirroring the bio-crude oil yield results and indicating the formation of aliphatic compounds from unsaturated and heteroatom-containing compounds from proteins and carbohydrates in *G. sulphuraria*. Different reaction conditions had little effect on the proton distribution for the HBO from *G. sulphuraria* (Table 8). LBO from *N. salina* contained more fatty acid-derived (0.5–1.5 ppm) and carbohydrate-derived (3.0–4.4 ppm and 4.4–6.0 ppm) compounds than LBO from *G. sulphuraria*, which contained more protein-derived compounds: straight/branched amides (1.5–3.0 ppm) and N-containing cyclic aromatics (6.0–8.8 ppm) (Fig. S18). Increasing the solid algae content from 5 wt.% to 10 wt.% had little effect on the proton distribution for either algae species (Fig. S19). Overall, ^1H NMR results were consistent with the results from FT-ICR MS: more O-containing compounds in *N. salina* bio-crude oils, more N-containing compounds in *G. sulphuraria* bio-crude oils, and more aromatic hetero-compounds with increasing reaction severity.

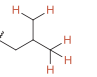
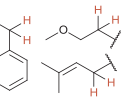
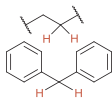
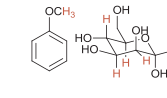
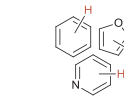
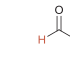
3.5. Biomass and bio-crude oil composition by FT-IR

FT-IR spectra for the algal biomass and the LBO produced at the conditions giving the highest oil yields are shown in Figs. 9 and 10. FT-IR spectra for LBO from HTL of both algae species (5 wt.%, 310 °C, 60 min) are compared in Fig. 11. Band assignments are based on [60,61].

Peak distributions for the two algal biomass samples are similar. The

Table 5

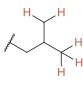
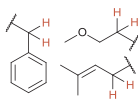
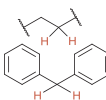
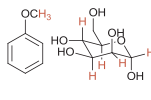
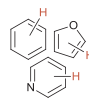
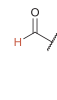
Proton type distribution in hexane-soluble LBO from HTL of *N. salina* under different operating conditions. Figures adapted from [56]. SAC = solid algae content.

Proton type		Aliphatic	Unsaturated/heteroatom	Alcohol/methylene-dibenzene/	Carbohydrate/unconjugated olefin	(Hetero-)aromatic	Aldehyde
							
		Range (ppm)					
Sample SAC wt. %	Log (R _t) ^a	0.5–1.5	1.5–3.0	3.0–4.4	4.4–6.0	6.0–8.0	9.0–10.1
5	7.35	52.03	17.98	5.26	7.66	12.74	4.33
5	7.78	51.53	18.48	5.33	7.55	12.88	4.21
5	8.03	46.96	17.11	8.95	8.89	13.51	4.59
10	8.03	47.24	18.73	6.56	8.33	14.75	4.39
5	8.62	48.82	18.54	6.05	7.99	14.13	4.46
5	9.21	46.59	17.58	7.79	9.84	13.58	4.62

^a Log (R_t) = 7.35, 7.78, 8.03, 8.62, and 9.21 correspond to HTL conditions of 310 °C and 5 min, 310 °C and 30 min, 310 °C and 60 min, 330 °C and 60 min, and 350 °C and 60 min, respectively.

Table 6

Proton type distribution in hexane-insoluble, DCM-soluble HBO from HTL of *N. salina* under different Log (R_t) (operating conditions). Figures adapted from [56]. SAC = solid algae content.

Proton type	Aliphatic	Unsaturated/heteroatom	Alcohol/methylene-dibenzene/	Carbohydrate/unconjugated olefin	(Hetero-)aromatic	Aldehyde	
							
Sample SAC wt.%	Log (R _t) ^a	Range (ppm)					
		0.5–1.5	1.5–3.0	3.0–4.4	4.4–6.0	6.0–8.0	9.0–10.1
5	7.35	29.29	28.84	10.60	9.41	16.58	5.29
5	7.78	30.64	27.32	11.26	9.22	16.41	5.15
5	8.03	27.79	28.95	11.01	8.29	18.39	5.57
10	8.03	27.44	28.47	10.78	9.85	17.83	5.63
5	8.62	18.93	28.16	12.17	12.37	21.19	7.18
5	9.21	19.97	23.05	13.46	13.20	22.66	7.65

^a Log (R_t) = 7.35, 7.78, 8.03, 8.62, and 9.21 correspond to HTL conditions of 310 °C and 5 min, 310 °C and 30 min, 310 °C and 60 min, 330 °C and 60 min, and 350 °C and 60 min, respectively.

main peaks include N–H stretching (3600–3300 cm^{-1}), C=O stretching (amide I band, 1634 cm^{-1}), and N–H bending (amide II band, 1545 cm^{-1}), indicating the presence of proteins. The C–H stretching (2955, 2922, and 2853 cm^{-1}), C=O stretching (1710.5 cm^{-1}), and C–H bending (1456.22 and 1376.92 cm^{-1}) peaks indicate the presence of lipids. When distinguishable, the C–O–C stretching peak (1188–900 cm^{-1}) indicates the presence of carbohydrates. The P=O stretching peak (1341–1188 cm^{-1}) is attributed to the phosphodiester in the algal nucleic acids and phospholipids. During HTL, N–H stretching, C=O stretching (lipids), C=O stretching (amide I band), N–H stretching (amide II band), P=O stretching, and C–O–C stretching peaks disappear (Figs. 9 and 10) as heteroatom-containing groups are eliminated. Simultaneously, C(sp³)–H stretching, C=O stretching (fatty acids), and C–H bending (saturated and unsaturated aliphatic structures) peaks appear to grow, implying the generation of fatty acids and heteroatom-containing unsaturated aliphatic and cyclic compounds. Formation of such compounds during HTL is supported by the FT-ICR data, and previously described HTL reaction pathways involving hydrolysis, dehydration, decarboxylation, decarbonylation, deamination, amidation, rearrangement, and aromatization [62,63].

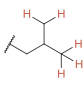
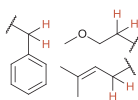
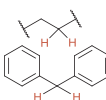
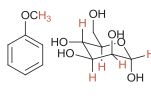
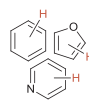
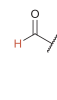
Comparing the LBO spectra from the two algae species, larger N–H stretching (3332 cm^{-1}), C=O (amide I band, 1657 cm^{-1}), N–H stretching (amide II band, 1516 cm^{-1}), and C–N stretching (1368 cm^{-1} and 1125–990 cm^{-1}) peaks were observed for *G. sulphuraria* LBO, indicating greater abundance of amines and amides in *G. sulphuraria* LBO due to the higher protein content. *N. salina* LBO had stronger C–H stretching (2955, 2922, and 2853 cm^{-1}) and C–O–H in-plane bending (1409 cm^{-1}) peaks relative to *G. sulphuraria* LBO, which

are attributed to the higher number of methylene and methyl groups in the greater fatty acid content in *N. salina* LBO, as supported by the FAME data. *N. salina* LBO also showed stronger absorbance in the C=O stretching region (1710–1705 cm^{-1}) than *G. sulphuraria* LBO, suggesting a greater abundance of unsaturated carboxylic acids from fatty acids. The C=O stretching that was observed for *G. sulphuraria* LBO was most likely from cyclic amides and/or carbonyl compounds produced by amidation, rearrangement, and Maillard reactions of proteins with lipids and carbohydrates in *G. sulphuraria* microalgae [14], as supported by the FT-ICR data. Both algal LBO had two clear C–H bending peaks (1456 and 1377 cm^{-1}) for aliphatic or cyclic structures. *G. sulphuraria* LBO had stronger absorbance for C=C stretching (1680–1560 cm^{-1}), which suggests more highly unsaturated aliphatic and cyclic structures. More carbohydrates in the *N. salina* biomass led to broader and stronger C–O stretching peaks (1320–1125 cm^{-1}). *N. salina* LBO had peaks corresponding to a greater amount of unsaturated aliphatic compounds: =C–H out-of-plane bending (vibrations at 990–835 cm^{-1}), while *G. sulphuraria* LBO had broader and stronger C(aromatic)–H out-of-plane bending peaks (835–600 cm^{-1}), indicating a greater amount of aromatic compounds, in agreement with the results of ¹H NMR and FT-ICR data for *G. sulphuraria* LBO.

Figs. 12 and 13 compare the FT-IR spectra for the HBO and LBO from *N. salina* and *G. sulphuraria*, respectively. For *N. salina*, the HBO had stronger and broader O–H and N–H stretching peaks (3300–2500 cm^{-1}) and C=C stretching peaks (1670–1540 cm^{-1}), indicating a greater abundance of heteroatom-containing unsaturated aliphatic or cyclic compounds in the HBO. The LBO had sharper and stronger C–H stretching (2955, 2922, and 2853 cm^{-1}), C=O stretching

Table 7

Proton type distribution in hexane-soluble LBOs from HTL of *G. sulphuraria* under different Log (R_t) (operating conditions). Figures adapted from [56]. SAC = solid algae content.

Proton type	Aliphatic	Unsaturated/heteroatom	Alcohol/methylene-dibenzene/	Carbohydrate/unconjugated olefin	(Hetero-)aromatic	Aldehyde	
							
Sample SAC wt.%	Log (R _t) ^a	Range (ppm)					
		0.5–1.5	1.5–3.0	3.0–4.4	4.4–6.0	6.0–8.0	9.0–10.1
5	8.03	51.70	20.17	5.59	6.49	12.34	3.72
5	8.55	39.23	23.73	8.12	8.60	15.30	5.03
5	8.62	43.98	21.22	7.19	8.23	14.94	4.45
5	8.97	39.71	23.94	7.94	8.23	15.51	4.66
5	9.21	45.51	20.08	6.76	7.49	15.65	4.51
10	9.21	42.35	22.66	7.18	7.47	15.93	4.42

^a Log (R_t) = 8.03, 8.55, 8.62, 8.97, and 9.21 correspond to HTL conditions of 310 °C and 60 min, 350 °C and 5 min, 330 °C and 60 min, 350 °C and 30 min, and 350 °C and 60 min, respectively.

Table 8

Proton type distribution in hexane-insoluble, DCM-soluble HBO from HTL of *G. sulphuraria* under different Log (R_t) (operating conditions). Figures adapted from [56]. SAC = solid algae content.

Proton type	Aliphatic	Unsaturated/heteroatom	Alcohol/methylene-dibenzene/	Carbohydrate/unconjugated olefin	(Hetero-)aromatic	Aldehyde	
Sample SAC wt. %	Log (R _t) ^a	Range (ppm)					
		0.5–1.5	1.5–3.0	3.0–4.4	4.4–6.0	6.0–8.0	9.0–10.1
5	8.03	24.97	28.85	11.92	9.40	19.45	5.41
5	8.55	23.86	31.09	11.77	8.94	19.19	5.15
5	8.62	25.90	26.48	13.46	9.07	19.86	5.23
5	8.97	22.07	32.08	11.57	9.52	19.29	5.46
5	9.21	22.77	29.70	11.35	10.09	20.02	6.08
10	9.21	22.90	32.50	11.32	8.80	19.12	5.37

^a Log (R_t) = 8.03, 8.55, 8.62, 8.97, and 9.21 correspond to HTL conditions of 310 °C and 60 min, 350 °C and 5 min, 330 °C and 60 min, 350 °C and 30 min, and 350 °C and 60 min, respectively.

(1710.5 cm^{-1}), and C–H bending (1457.5 cm^{-1}) peaks, indicating the larger amount of fatty acids. For *G. sulphuraria*, the HBO had broader and stronger O–H and N–H stretching (3300–2500 cm^{-1}), C=C stretching (1605–1551 cm^{-1}), N–H bending (1513 cm^{-1}), C–O bending (1267–1168 cm^{-1}), and C–H bending (741 cm^{-1}) peaks, indicating the greater abundance of heteroatom-containing unsaturated aliphatic and aromatic compounds in HBO, as was observed for *N. salina* HBO. The greater abundance of these heteroatom-containing cyclic compounds suggests that upgrading HBO would be more difficult than upgrading LBO, regardless of algal species.

For a given algae species, different HTL temperatures, reaction times, and solid algae loadings had little effect on the functional groups observable by FT-IR, as shown in [supplemental information Figs. S20–S25](#).

3.6. Coupling HTL conditions to bio-crude oil upgrading

Catalytic upgrading of algae HTL bio-crude oils to “drop-in” transportation fuels faces four main challenges: ash, oxygen, nitrogen, and polycyclic aromatic compounds. In bio-crude oil from HTL of a low-

lipid, high-protein algae like *G. sulphuraria*, more severe reaction conditions tend to create compounds that contain oxygen, nitrogen, AND are polycyclic aromatic—a unfortunate synergy. FT-ICR MS analysis indicates that *G. sulphuraria* LBO contains more low-DBE hetero-compounds than *N. salina* LBO for a given compound class, even though *N. salina* LBO has lower concentrations of hetero-compounds overall. The higher-DBE hetero-compounds are likely due to carbohydrate content, which undergoes rearrangement and repolymerization of carbohydrate-derived furfurals into recalcitrant aromatic structures [64,65]. Extraction of carbohydrates (and ash) prior to HTL has been shown to improve oil production and inhibit char formation [46,66]. With less participation of carbohydrate derivatives in HTL, protein-derived intermediates are less likely to form multi-ring aromatics [67]. Therefore, the nitrogen present in bio-crude oil from HTL of high-protein algae biomass would be an aliphatic form and could be more easily removed in downstream catalytic upgrading. In addition, carbohydrates could be recycled to produce polysaccharides, a potential bio-resource of value-added products [46].

Just as carbohydrates can be extracted from algal biomass prior to HTL, methods could be developed to extract proteins from algal

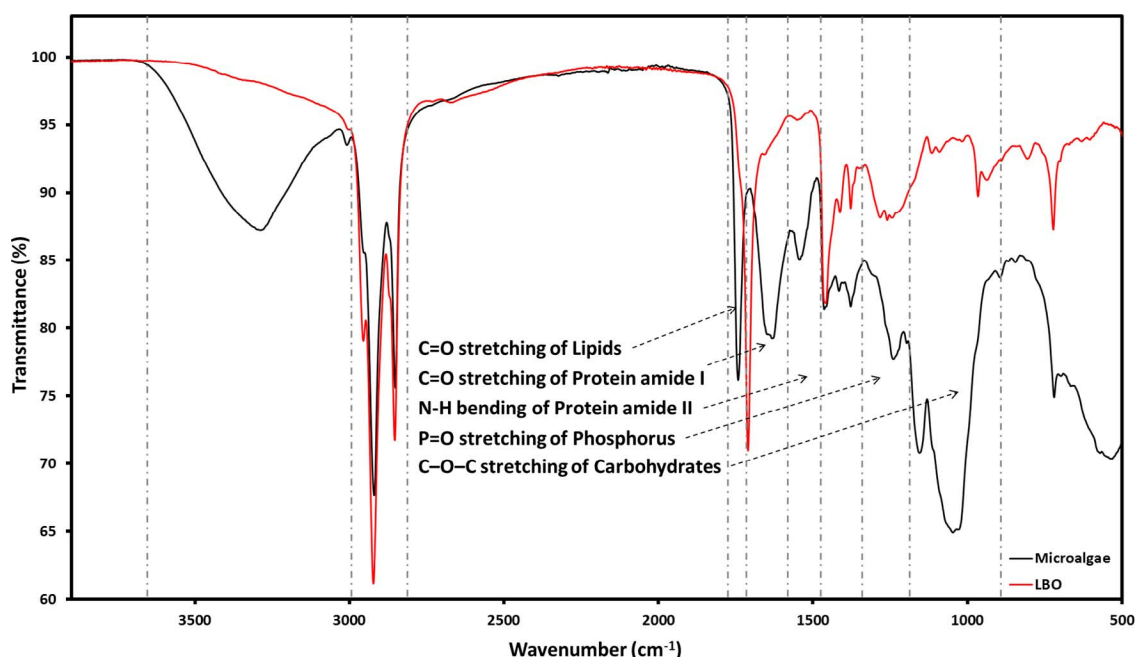


Fig. 9. FT-IR spectra of *N. salina* biomass and LBO produced under the conditions giving the highest oil yield (5 wt.% solids, 310 °C, 60 min).

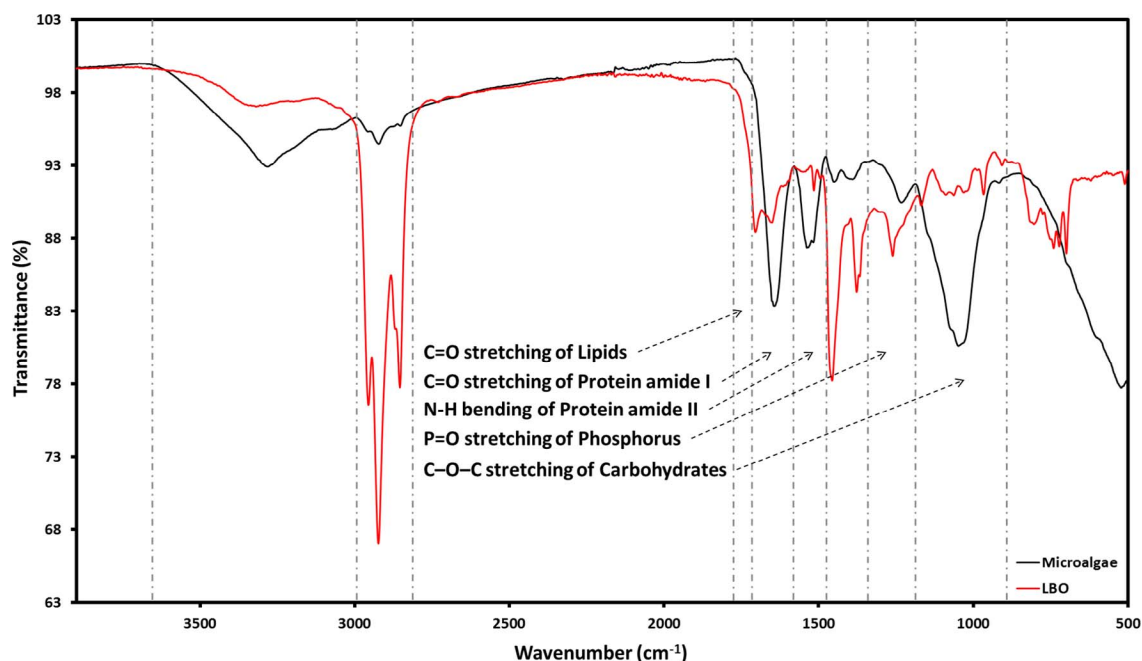


Fig. 10. FT-IR spectra of *G. sulphuraria* biomass and LBO produced under the conditions giving the highest oil yield (5 wt.% solids, 350 °C, 60 min).

biomass prior to HTL. An argument in favor of protein extraction is the reduction in denitrogenation required during upgrading. For high-protein algae like *G. sulphuraria*, two arguments could be made to remove nitrogen by downstream catalytic denitrogenation rather than protein removal pretreatment: overall yield of HTL bio-crude oil and fatty-acid amide stability. To date, few studies on efficient nitrogen extraction prior to HTL are available [68,69]. Based on the substantial fraction in bio-crude oil that is protein-derived, there is a dramatic reduction in oil yield after nitrogen removal [70], such that HTL of high-protein algae like *G. sulphuraria* would be impractical for any kind of energy recovery. Results from FAME-GC and ^1H NMR analyses suggest that energy-rich fatty acid content increases with higher temperatures and longer reaction times in *G. sulphuraria*-derived LBO. As reaction condition severity increases, proteins are incorporated into the

bio-crude oil phase and react with fatty acids to form relatively stable fatty acid amides [65] (due to electron delocalization on the nitrogen by resonance [71]), thereby generating more aliphatic (rather than aromatic) structures that are easier to upgrade.

The most effective pathway forward for recovery of transportation fuels from HTL of high-protein, low-lipid algae is, therefore, likely to be a three-step process: (1) low temperature (< 200 °C) hydrothermal pretreatment of the algal feedstock to remove ash and carbohydrates, (2) higher temperature subcritical (330–360 °C) HTL of the pretreated algal feedstock containing mostly proteins and lipids, and (3) catalytic denitrogenation of the bio-crude oils [72,73], prior to final upgrading.

In addition, using a less polar solvent such as hexane for the bio-crude oil recovery will reduce overall yields but will also decrease the number of heteroatoms and high-molecular weight compounds in the

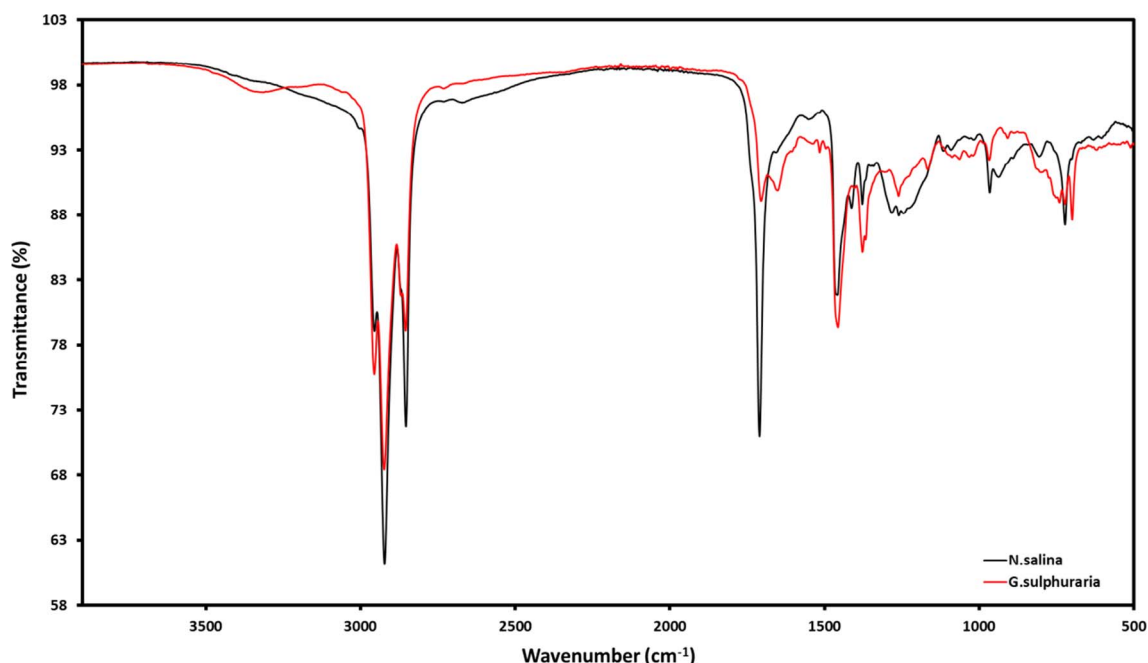


Fig. 11. FT-IR spectra of LBO produced from HTL of 5 wt.% *N. salina* and *G. sulphuraria* at 310 °C and 60 min.

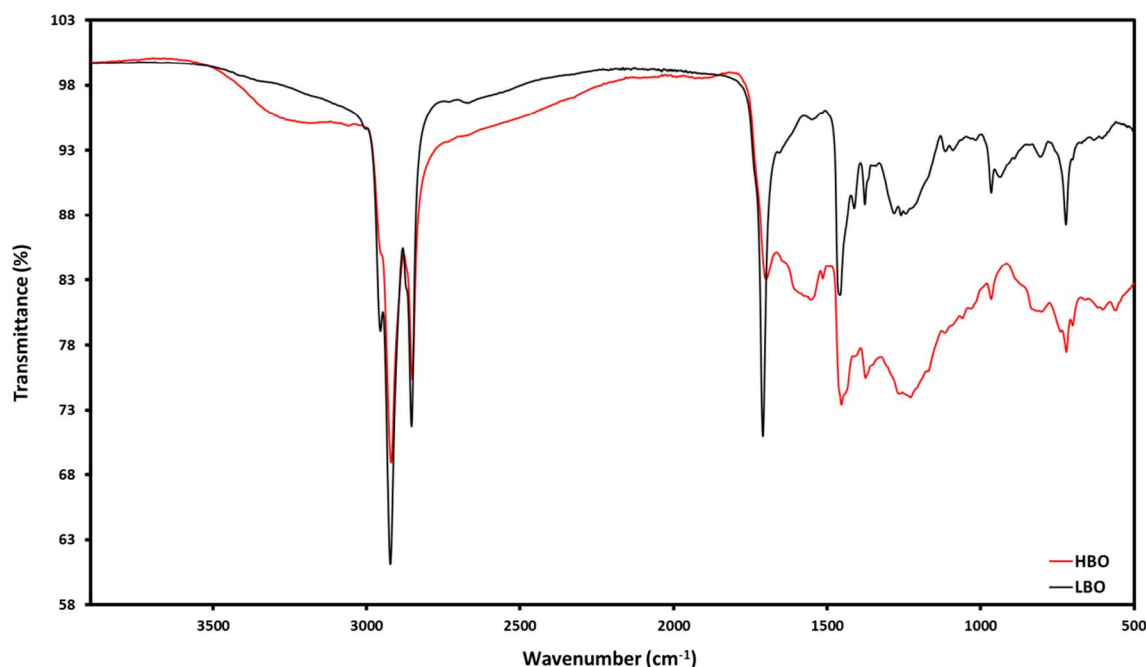


Fig. 12. FT-IR spectra of LBO and HBO produced from HTL of 5 wt.% *N. salina* at 310°C and 60 min.

bio-crude oil that is sent for upgrading. FT-ICR MS analysis is likely to be a helpful tool for monitoring bio-crude oil chemistry improvements (decrease in multiple-heteroatom content and decrease in DBE) with pretreatment and HTL reaction condition optimization studies.

4. Conclusions

Characterization of bio-crude oils derived from the hydrothermal liquefaction of a low-lipid, high-protein microalgae *G. sulphuraria* compared to bio-crude oil derived from a typical lipid-rich microalgae showed that milder operating conditions (e.g. 310 °C) favor bio-crude oil yield and quality for lipid-rich algae, while more severe conditions (e.g. 350 °C) are needed for high-protein algae. Hexane-soluble bio-

crude oil from *N. salina* contains more fatty-acid-derived and O-containing compounds, while bio-crude oil from *G. sulphuraria* contains greater amounts of N heteroatom-containing cyclic compounds due to the higher protein content. While high-protein algae like *G. sulphuraria* represent less favorable feedstocks for bio-crude oil production, their faster growth rates, their greater tolerance of “field” growth conditions, and their potential for use in wastewater treatment may outweigh the bio-crude oil yield and quality limitations. Removal of carbohydrates through a low temperature pretreatment may improve bio-crude oil quality for downstream upgrading by decreasing the interactions of protein-derived and carbohydrate-derived compounds during HTL that form the highly aromatic compounds containing multiple heteroatoms. Future work in catalyst development for utilization of high-protein

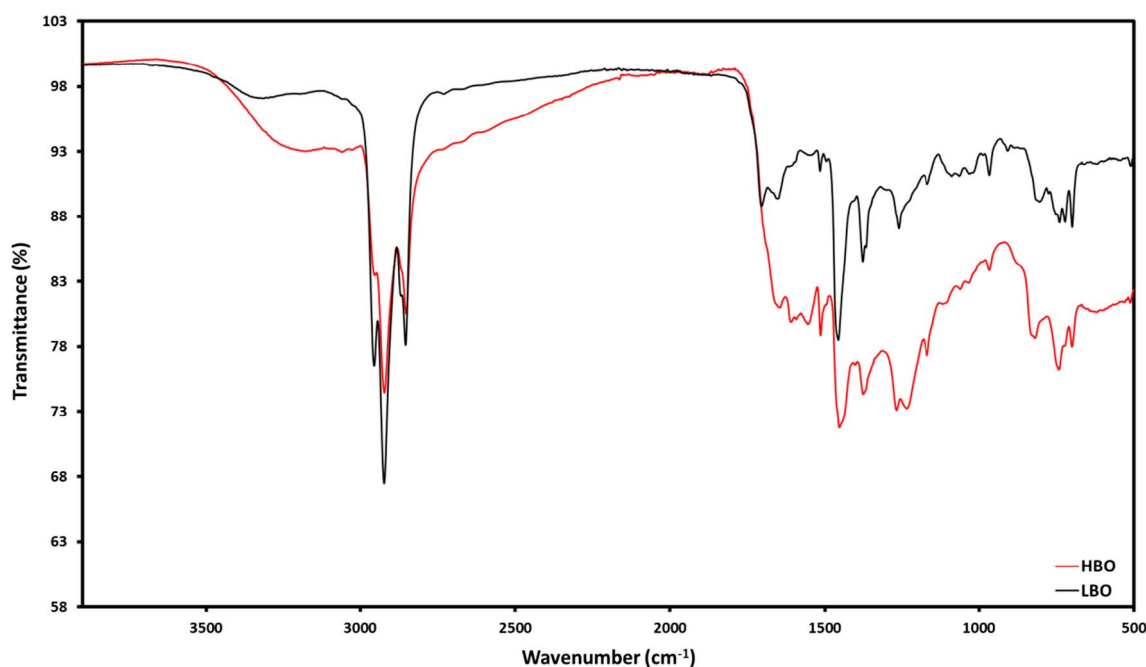


Fig. 13. FT-IR spectra of LBO and HBO produced from HTL of 5 wt.% *G. sulphuraria* at 350 °C and 60 min.

algal biomass should focus on bimetallic catalysts that can crack larger bio-crude oil compounds and remove nitrogen heteroatoms [74].

Acknowledgements

The authors acknowledge funding from the National Science Foundation “ReNUWIT” Energy Research Center (#1028968), the National Science Foundation New Mexico EPSCOR Research Infrastructure Improvement grant “Energy New Mexico” (#1031346), NSF Major Research Instrumentation Program (NSF MRI 1626468), the U.S. Department of Energy Regional Algal Fuels Testbed Partnership (#DE-EE0006269), the Center for Animal Health and Food Safety at NMSU and the NMSU Ed & Harold Foreman Endowed Chair. The authors also acknowledge assistance from members of the Holguin, Van Voohries, Boeing, Khandan, and Brewer research groups during algae production, harvesting, conversion, and characterization, as well as NMR data interpretation assistance from J.W. Herndon.

Appendix A. Supplementary material

Supplementary data associated with this article can be found, in the online version, at <http://dx.doi.org/10.1016/j.apenergy.2017.08.105>.

References

- Libra JA, Ro KS, Kammann C, Funke A, Berge ND, Neubauer Y, et al. Hydrothermal carbonization of biomass residuals: a comparative review of the chemistry, processes and applications of wet and dry pyrolysis. *Biofuels* 2011;2:71–106.
- Matsumura Y, Minowa T, Potic B, Kersten SR, Prins W, van Swaaij WP, et al. Biomass gasification in near-and super-critical water: status and prospects. *Biomass Bioenerg* 2005;29:269–92.
- Kumar A. A conceptual comparison of biopower generation options. In: 2006 ASAE annual meeting: american society of agricultural and biological engineers; 2006. p. 1.
- Yu G, Zhang Y, Schideman L, Funk T, Wang Z. Distributions of carbon and nitrogen in the products from hydrothermal liquefaction of low-lipid microalgae. *Energy Environ Sci* 2011;4:4587–95.
- Jena U, Das K, Kastner J. Effect of operating conditions of thermochemical liquefaction on biocrude production from *Spirulina platensis*. *Bioresour Technol* 2011;102:6221–9.
- Bach Q-V, Sillero MV, Tran K-Q, Skjermo J. Fast hydrothermal liquefaction of a Norwegian macro-alga: screening tests. *Algal Res* 2014;6:271–6.
- Duan P, Savage PE. Catalytic treatment of crude algal bio-oil in supercritical water: optimization studies. *Energy Environ Sci* 2011;4:1447–56.
- Peterson AA, Vogel F, Lachance RP, Fröling M, Antal Jr MJ, Tester JW. Thermochemical biofuel production in hydrothermal media: a review of sub-and supercritical water technologies. *Energy Environ Sci* 2008;1:32–65.
- Savage P, Levine R, Huelsman C. Hydrothermal processing of biomass. In: Crocker M, editor. *Thermochemical conversion of biomass to liquid fuels and chemicals*. Royal Soc. Chem. Publishing; 2010. p. 192–221.
- Shakya R, Whelen J, Adhikari S, Mahadevan R, Neupane S. Effect of temperature and Na_2CO_3 catalyst on hydrothermal liquefaction of algae. *Algal Res* 2015;12:80–90.
- Yang C, Jia L, Chen C, Liu G, Fang W. Bio-oil from hydro-liquefaction of *Dunaliella salina* over Ni/REHY catalyst. *Bioresour Technol* 2011;102:4580–4.
- Huang H, Yuan X, Zeng G, Wang J, Li H, Zhou C, et al. Thermochemical liquefaction characteristics of microalgae in sub-and supercritical ethanol. *Fuel Process Technol* 2011;92:147–53.
- Duan P, Bai X, Xu Y, Zhang A, Wang F, Zhang L, et al. Catalytic upgrading of crude algal oil using platinum/gamma alumina in supercritical water. *Fuel* 2013;109:225–33.
- Zhang C, Tang X, Sheng L, Yang X. Enhancing the performance of co-hydrothermal liquefaction for mixed algae strains by the Maillard reaction. *Green Chem* 2016;18:2542–53.
- Sato N, Quitain AT, Kang K, Daimon H, Fujie K. Reaction kinetics of amino acid decomposition in high-temperature and high-pressure water. *Ind Eng Chem Res* 2004;43:3217–22.
- Demirbas MF. Biofuels from algae for sustainable development. *Appl Energy* 2011;88:3473–80.
- Toor SS, Rosendahl L, Rudolf A. Hydrothermal liquefaction of biomass: a review of subcritical water technologies. *Energy* 2011;36:2328–42.
- Li Y, Leow S, Fedders AC, Sharma BK, Guest JS, Strathmann TJ. Quantitative multiphase model for hydrothermal liquefaction of algal biomass. *Green Chem* 2017;19:1163–74.
- Garcia Alba L, Torri C, Samori C, van der Spek J, Fabbri D, Kersten SR, et al. Hydrothermal treatment (HTT) of microalgae: evaluation of the process as conversion method in an algae biorefinery concept. *Energy Fuels* 2011;26:642–57.
- Torri C, Garcia Alba L, Samori C, Fabbri D, Brilman DW. Hydrothermal treatment (HTT) of microalgae: detailed molecular characterization of HTT oil in view of HTT mechanism elucidation. *Energy Fuels* 2012;26:658–71.
- Hughey CA, Rodgers RP, Marshall AG. Resolution of 11,000 compositionally distinct components in a single electrospray ionization Fourier transform ion cyclotron resonance mass spectrum of crude oil. *Anal Chem* 2002;74:4145–9.
- Leonardi I, Chiaberge S, Fiorani T, Spera S, Battistel E, Bosetti A, et al. Characterization of bio-oil from hydrothermal liquefaction of organic waste by NMR spectroscopy and FTICR mass spectrometry. *ChemSusChem* 2013;6:160–7.
- Holguin FO, Schaub T. Characterization of microalgal lipid feedstock by direct-infusion FT-ICR mass spectrometry. *Algal Res* 2013;2:43–50.
- Sudasinghe N, Dungan B, Lammers P, Albrecht K, Elliott D, Hallen R, et al. High resolution FT-ICR mass spectral analysis of bio-oil and residual water soluble organics produced by hydrothermal liquefaction of the marine microalga *Nannochloropsis salina*. *Fuel* 2014;119:47–56.
- Rodgers RP, Schaub TM, Marshall AG. Petroleomics: MS returns to its roots. *Anal Chem* 2005;77. 20 A-7 A.
- Fernandez-Lima FA, Becker C, McKenna AM, Rodgers RP, Marshall AG, Russell DH. Petroleum crude oil characterization by IMS-MS and FTICR MS. *Anal Chem* 2009;81:9941–7.
- Jarvis JM, McKenna AM, Hiltner RN, Das K, Rodgers RP, Marshall AG. Characterization of pine pellet and peanut hull pyrolysis bio-oils by negative-ion electrospray ionization Fourier transform ion cyclotron resonance mass spectrometry. *Energy Fuels* 2012;26:3810–5.
- Vardon DR, Sharma BK, Blazina GV, Rajagopalan K, Strathmann TJ. Thermochemical conversion of raw and defatted algal biomass via hydrothermal liquefaction and slow pyrolysis. *Biores Technol* 2012;109:178–87.
- Sudasinghe N, Cort JR, Hallen R, Olarte M, Schmidt A, Schaub T. Hydrothermal liquefaction oil and hydrotreated product from pine feedstock characterized by heteronuclear two-dimensional NMR spectroscopy and FT-ICR mass spectrometry. *Fuel* 2014;137:60–9.
- Rodolfi G, Zittelli GC, Bassi N, Padovani G, Biondi N, Bonini G. Microalgae for oil: strain selection, induction of lipid synthesis and outdoor mass cultivation in a low-cost photobioreactor. *J Ind Microbiol Biotechnol* 2009;36:269–74.
- Selvaratnam T, Pegallapati A, Montoya F, Rodriguez N, Nirmalakhandan N, Van Voohries W. Evaluation of a thermo-tolerant acidophilic alga, *Galdieria sulphuraria*, for nutrient removal from urban wastewaters. *Biores Technol* 2014;156:395–9.
- Ledford Jr EB, Rempel DL, Gross M. Space charge effects in Fourier transform mass spectrometry II. Mass calibration. *Anal Chem* 1984;56:2744–8.
- Corilo YE. *PetroOrg Software*. Florida State University. All rights reserved.
- Kendrick E. A mass scale based on $\text{CH}_2 = 14.0000$ for high resolution mass spectrometry of organic compounds. *Anal Chem* 1963;35:2146–54.
- Mayers JJ, Flynn KJ, Shields RJ. Rapid determination of bulk microalgal biochemical composition by Fourier-transform infrared spectroscopy. *Biores Technol* 2013;148:215–20.
- Valdez PJ, Nelson MC, Wang HY, Lin XN, Savage PE. Hydrothermal liquefaction of *Nannochloropsis* sp.: systematic study of process variables and analysis of the product fractions. *Biomass Bioenerg* 2012;46:317–31.
- Peterson AA, Lachance RP, Tester JW. Kinetic evidence of the Maillard reaction in hydrothermal biomass processing: glucose–glycine interactions in high-temperature, high-pressure water. *Ind Eng Chem Res* 2010;49:2107–17.
- Luijckx GC, van Rantwijk F, van Bekkum H. Hydrothermal formation of 1, 2, 4-benzenetriol from 5-hydroxymethyl-2-furaldehyde and D-fructose. *Carbohydr Res* 1993;242:131–9.
- Dandamudi KPR, Muppaneni T, Sudasinghe N, Schaub T, Holguin FO, Lammers PJ, et al. Co-liquefaction of mixed culture microalgal strains under sub-critical water conditions. *Biores Technol* 2017;236:129–37.
- Toor SS, Reddy H, Deng S, Hoffmann J, Spangsmark D, Madsen LB, et al. Hydrothermal liquefaction of *Spirulina* and *Nannochloropsis salina* under sub-critical and supercritical water conditions. *Bioresour Technol* 2013;131:413–9.
- Jarvis JM, Billing JM, Hallen RT, Schmidt AJ, Schaub TM. Hydrothermal liquefaction biocrude compositions compared to petroleum crude and shale oil. *Energy Fuels* 2017;31:2896–906.
- Brown TM, Duan P, Savage PE. Hydrothermal liquefaction and gasification of *Nannochloropsis* sp. *Energy Fuels* 2010;24:3639–46.
- Knezevic D, Van Swaaij W, Kersten S. Hydrothermal conversion of biomass: I, glucose conversion in hot compressed water. *Ind Eng Chem Res* 2009;48:4731–43.
- Simoneit BR, Rushdi A, Bin Abas M, Didyk B. Alkyl amides and nitriles as novel tracers for biomass burning. *Environ Sci Technol* 2003;37:16–21.
- Chen Y, Zhao N, Wu Y, Wu K, Wu X, Liu J, et al. Distributions of organic compounds to the products from hydrothermal liquefaction of microalgae. *Environ Prog Sust Energy* 2017;36:259–68.
- Miao C, Chakraborty M, Chen S. Impact of reaction conditions on the simultaneous production of polysaccharides and bio-oil from heterotrophically grown *Chlorella sorokiniana* by a unique sequential hydrothermal liquefaction process. *Bioresour Technol* 2012;110:617–27.
- Madsen RB, Zhang H, Biller P, Goldstein AH, Glasius M. Characterizing semivolatile organic compounds of bio-crude from hydrothermal liquefaction of biomass. *Energy Fuels* 2017;31:4122–34.
- Pedersen TH, Rosendahl LA. Production of fuel range oxygenates by supercritical hydrothermal liquefaction of lignocellulosic model systems. *Biomass Bioenerg* 2015;83:206–15.
- Tang X, Zhang C, Li Z, Yang X. Element and chemical compounds transfer in bio-crude from hydrothermal liquefaction of microalgae. *Bioresour Technol* 2016;202:8–14.
- Yang W, Li X, Li Z, Tong C, Feng L. Understanding low-lipid algae hydrothermal liquefaction characteristics and pathways through hydrothermal liquefaction of

- algal major components: crude polysaccharides, crude proteins and their binary mixtures. *Bioresour Technol* 2015;196:99–108.
- [51] Vo TK, Lee OK, Lee EY, Kim CH, Seo J-W, Kim J, et al. Kinetics study of the hydrothermal liquefaction of the microalga *Aurantiochytrium* sp. KRS101. *Chem Eng J* 2016;306:763–71.
- [52] Carey FA. *Organic chemistry*. 6th ed. New York: McGraw-Hill; 2006.
- [53] Wang X, Sheng L, Yang X. Pyrolysis characteristics and pathways of protein, lipid and carbohydrate isolated from microalgae *Nannochloropsis* sp. *Biores Technol* 2017.
- [54] Gai C, Zhang Y, Chen W-T, Zhang P, Dong Y. An investigation of reaction pathways of hydrothermal liquefaction using *Chlorella pyrenoidosa* and *Spirulina platensis*. *Energy Convers Manage* 2015;96:330–9.
- [55] Patil PD, Reddy H, Muppaneni T, Deng S. Biodiesel fuel production from algal lipids using supercritical methyl acetate (glycerin-free) technology. *Fuel* 2017;195:201–7.
- [56] Mullen CA, Strahan GD, Boateng AA. Characterization of various fast-pyrolysis bio-oils by NMR spectroscopy†. *Energy Fuels* 2009;23:2707–18.
- [57] Gai C, Zhang Y, Chen W-T, Zhang P, Dong Y. Energy and nutrient recovery efficiencies in biocrude oil produced via hydrothermal liquefaction of *Chlorella pyrenoidosa*. *RSC Adv* 2014;4:16958–67.
- [58] Özbay N, Apaydin-Varol E, Uzun BB, Pütün AE. Characterization of bio-oil obtained from fruit pulp pyrolysis. *Energy* 2008;33:1233–40.
- [59] Ingram L, Mohan D, Bricka M, Steele P, Strobel D, Crocker D, et al. Pyrolysis of wood and bark in an auger reactor: physical properties and chemical analysis of the produced bio-oils. *Energy Fuels* 2007;22:614–25.
- [60] Murdock JN, Wetzel DL. FT-IR microspectroscopy enhances biological and ecological analysis of algae. *Appl Spectrosc Rev* 2009;44:335–61.
- [61] Villacorte LO, Ekowati Y, Neu TR, Kleijn JM, Winters H, Amy G, et al. Characterisation of algal organic matter produced by bloom-forming marine and freshwater algae. *Water Res* 2015;73:216–30.
- [62] Bobleter O. Hydrothermal degradation of polymers derived from plants. *Prog Polym Sci* 1994;19:797–841.
- [63] Kruse A, Dinjus E. Hot compressed water as reaction medium and reactant: Properties and synthesis reactions. *J Supercrit Fluids* 2007;39:362–80.
- [64] Guo Y, Yeh T, Song W, Xu D, Wang S. A review of bio-oil production from hydrothermal liquefaction of algae. *Renew Sustain Energy Rev* 2015;48:776–90.
- [65] Kumar G, Shobana S, Chen W-H, Bach Q-V, Kim S-H, Atabani A, et al. A review of thermochemical conversion of microalgal biomass for biofuels: chemistry and processes. *Green Chem* 2017;19:44–67.
- [66] Chakraborty M, Miao C, McDonald A, Chen S. Concomitant extraction of bio-oil and value added polysaccharides from *Chlorella sorokiniana* using a unique sequential hydrothermal extraction technology. *Fuel* 2012;95:63–70.
- [67] Zhang J, Chen W-T, Zhang P, Luo Z, Zhang Y. Hydrothermal liquefaction of *Chlorella pyrenoidosa* in sub- and supercritical ethanol with heterogeneous catalysts. *Bioresour Technol* 2013;133:389–97.
- [68] Jazrawi C, Biller P, He Y, Montoya A, Ross AB, Maschmeyer T, et al. Two-stage hydrothermal liquefaction of a high-protein microalga. *Algal Res* 2015;8:15–22.
- [69] Eboibi B, Lewis DM, Ashman PJ, Chinnasamy S. Influence of process conditions on pretreatment of microalgae for protein extraction and production of biocrude during hydrothermal liquefaction of pretreated *Tetraselmis* sp. *RSC Adv* 2015;5:20193–207.
- [70] Costanzo W, Jena U, Hilten R, Das K, Kastner JR. Low temperature hydrothermal pretreatment of algae to reduce nitrogen heteroatoms and generate nutrient recycle streams. *Algal Res* 2015;12:377–87.
- [71] Dewick PM. *Essentials of organic chemistry: for students of pharmacy, medicinal chemistry and biological chemistry*. Hoboken, NJ: Wiley; 2013.
- [72] Wang Z, Adhikari S, Valdez P, Shakya R, Laird C. Upgrading of hydrothermal liquefaction biocrude from algae grown in municipal wastewater. *Fuel Process Technol* 2016;142:147–56.
- [73] Costanzo W, Hilten R, Jena U, Das K, Kastner JR. Effect of low temperature hydrothermal liquefaction on catalytic hydrodenitrogenation of algae biocrude and model macromolecules. *Algal Res* 2016;13:53–68.
- [74] Yang C, Li R, Cui C, Liu S, Qiu Q, Ding Y, et al. Catalytic hydroprocessing of microalgae-derived biofuels: a review. *Green Chem* 2016;18:3684–99.